MATERIALS PHYSICS AND MECHANICS RESEARCH ARTICLE

Submitted: December 10, 2025 **Revised: March 1, 2026** **Accepted: May 9, 2026**

Synthesis and characterization of corn starch based biodegradable plastic: microstructural, structural, and decomposition studies for potential applications

L. Srinivasa Rao [1] ✉, Jyotsna Cherukuri [1], N. Pothanna [1], R. Vijaya Saraswathi [1], L. Prabhatha Sindu Sri [2], Sahith Battula [1,3]

[1] VNR Vignana Jyothi Institute of Engineering and Technology, Hyderabad, Telangana, India

[2] B.V. Raju Institute of Technology, Narsapur, Telangana, India

[3] Ruhr-University Bochum, Bochum, Germany

✉ srinivasarao_l@vnrvjiet.in

ABSTRACT

This study focuses on the synthesis and characterization of biodegradable plastics using corn flour, vinegar, glycerin, and varying amounts of water. The biodegradable plastics were synthesized via a two-step process involving solvent casting and controlled physical foaming. X-ray diffraction patterns exhibited broad amorphous halos centered at $2\theta \approx 19.6°$, alongside weak peaks at 15.1 and 23.3°, indicating a semi-crystalline nature. Scanning electron microscopy displayed a heterogeneous grain surface of starch granules with an average pore size of ~ 119–585 μm^2. The prepared biodegradable plastics have the highest porosity (~ 31.67 %), depicting a loosely packed amorphous nature. Energy dispersion spectroscopy provided the elemental analysis of starch-based biopolymers. Fourier-transform infrared spectra showcased functional groups viz., hydroxyl (O–H) at ~ 3340–3365 cm^{-1}, carbonyl (C=O) at ~ 1717–1735 cm^{-1}, and glycosidic linkages (α-1,4) at ~ 917–926 cm^{-1}. The bioplastic samples have considerable degradation (up to 84.298 %) in red soil in a week. Thus, such starch-based bioplastics can be used as alternatives to conventional plastics.

KEYWORDS

bioplastics • solution casting • U-net model • porosity • FTIR spectra • biodegradability

Acknowledgements. *The authors would like to thank management of VNRVJIET for their encouragement.*

Citation: Srinivasa Rao L, Jyotsna C, Pothanna N, Vijaya Saraswathi R, Prabhatha Sindu Sri L, Sahith B. Synthesis and characterization of corn starch based biodegradable plastic: microstructural, structural, and decomposition studies for potential applications. *Materials Physics and Mechanics*. 2026;54(3): 104–119. http://dx.doi.org/10.18149/MPM.5432026_9

Introduction

The international production of plastics has exceeded ~436 million tons in 2022, of which more than 50 % could be exploited due to one-time use and short-term applications like packing, agri-films, and disposable goods [1]. Petroleum-based plastics cannot be degradable through microbial activity, and they cause environmental disruption and environmental pollution [2]. Only ~9% of plastic waste is being recycled, and rest of plastic waste accumulates in the natural environment (like landfills, drainage canals, revers, oceans, etc.), prompting the need of biodegradable alternatives. Biodegradable plastics derived from natural polymers such as starch [3,4], cellulose [4], chitosan [5], and polylactic acid (PLA) [6,7] have gained significant traction due to their ability to degrade under composting or microbial action. Among these, corn starch is particularly attractive

© L. Srinivasa Rao, Ch. Jyotsna, N. Pothanna, R. Vijaya Saraswathi, L. Prabhatha Sindu Sri, B. Sahith, 2026.
Publisher: Peter the Great St. Petersburg Polytechnic University
This is an open access article under the CC BY-NC 4.0 license (https://creativecommons.org/li-censes/by-nc/4.0/)

due to its abundant availability, low cost, non-toxicity, film-forming ability, and biodegradability [8]. Cornstarch-based bioplastics incorporating fructose and varying TiO_2 concentrations (0–0.3 g) have been investigated and identified that the bioplastic with 0.1 g TiO_2 has the smallest crystal size (12.54 nm), high water absorption (66.66 % after 120 s), and 80% biodegradation after 28 days [9]. Optimized edible films were made from extruded corn starch, gelatin (0–10 %), and glycerol via a casting process, finding that 2.93% gelatin and 80 °C extrusion temperature yielded the films with optimal tensile strength (8.34 MPa), elongation (25.60 %), and solubility (66.29–80.50 %) [10]. Thermal degradability of corn starch-based plastic plates via thermogravimetric analysis (TGA) with the rate of 10–100 °C/min has been observed, identifying two decomposition stages at temperatures of 250–620 °C and 620–855 °C with activation energies of 120.70 and 140.77 kJ/mol, respectively [11]. Biodegradable films were made from carrageenan powder (supplied by LP. Karagen Indonesia) and commercial corn starch blends (Bola Deli brand), processed through extrusion at 110 °C and compression molding at 160 °C, and observed that increased starch content improved strength, flexibility, and barrier properties, while carrageenan enhanced biodegradability, highlighting their potential for packaging applications [12]. The gelatinization process helped to prepare different types of biodegradable films by modifying the structure of starch granules [13].

Even though a greater number of studies on biodegradable plastics are available, some challenges persist for achieving good mechanical strength, more flexibility, and high water-resistance suitable for commercial packing applications. Further, there are several limitations on technical aspects like processing methods, blend compositions, long-term biodegradability, and performance of the bioplastics under varied environmental conditions. Usually, starch biofilms are highly brittle and poorly water- resistant. They have low thermal stability. Thus, starch biofilms have no commercial viability. A strategy to overcome such drawbacks is to develop porosity in the films. The porosity of biofilms could not only decrease density, but also increase flexibility, surface area, water diffusion capacity, and microbial activity during the degradation process [14]. Recent techniques available to fabricate porous starch-based bioplastics are physical foaming at the melting temperature (t_m) ~ 190–200 °C with lower water (H_2O) content (~ 10–30 %) [15], solvent casting with high content of a plasticizer (50% of glycerine) [16], and few other extraction methods [10,12,17]. The corn-starch bioplastic films were prepared using gelatin and glycerol by combined extrusion (at 80–120 °C) and casting processes at room temperature [10]. The carrageenan/corn based biodegradable plastic films were produced by extrusion at 110 °C, followed by hot compression at 160 ° [12]. The preparation of corn-starch blends has been accomplished through a sequence of multiple processes such as extraction at ~ 50–70 °C, washing at ~ 25–30 °C, and drying at ~ 40–60 °C [17].

The increasing environmental pollution caused by the petroleum-based plastics has twisted an essential need for alternative materials for daily life applications. The normal plastics could be accumulated in to landfills and ecosystems, which leads to long-term pollution, micro-plastic formation, and environmental destruction. In this way, the scope of this study on biodegradable plastics is to synthesis biomaterials that can be decomposed naturally through microbial action without leaving toxic residues. The key objectives include understanding the synthesis, microstructure, and structural properties of corn-based biodegradable plastics useful for packing and other potential applications.

Materials and Methods

Synthesis of samples

Commercially available corn flour (starch from corn, linear formula: $(C_6H_{10}O_5)_n$, CAS number: 9005-25-8) was used as the starch source. Glycerin (glycerol, linear formula: $HOCH_2CH(OH)CH_2OH$, CAS number: 56-81-5, purity ⩾ 99.0 %), vinegar (La Nature's Distilled White Vinegar, Manufacturer: Brio Vinegars, Haryana, India) and distilled water (H_2O) were used throughout the synthesis. The compositions for three formulations (BP-1, BP-2, and BP-3) are presented in Table 1.

Table 1. Composition of prepared cornstarch based biodegradable plastic (BP) samples

Sample	Corn flour, g	Vinegar, ml	Glycerin, ml	Water, ml
BP-1	15	10	10	30
BP-2	15	10	10	60
BP-3	15	10	10	90

The biodegradable plastics were synthesized via a two-step process involving solvent casting and controlled physical foaming [15,16]. This process involves four stages: (i) solution preparation, (ii) heating and gelatinization, (iii) casting and drying, and (iv) extraction of final samples, as shown in Fig. 1(a–d), respectively.

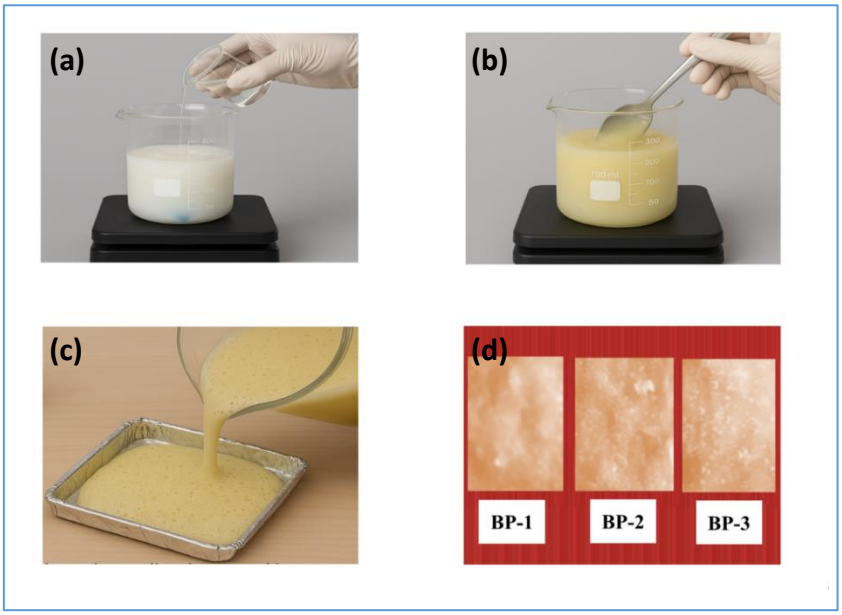


Fig. 1. An illustration of the preparation of corn starch-based bioplastics: (a) solution preparation; (b) heating and gelatinization; (c) gel spread into an aluminium foil; (d) final sample of biodegradable plastic

A fixed quantity of 15 g corn flour was first dispersed in the specified volume of distilled water (30, 60, or 90 ml) at room temperature. 10 ml of vinegar (as an acidifier to reduce pH and initiate gelatinization) and 10 ml of glycerin (as a plasticizer) were added to the dispersion. The mixture was stirred vigorously for 10 min using a magnetic stirrer to ensure formation of a uniform solution in a borosil beaker, as shown in Fig. 1(a). The pre-mixed solution was transferred into another borosil beaker and heated over a hot plate at 85 ± 2 °C for 25–30 min, under constant mechanical stirring at 500 rpm. During heating,

starch gelatinization occurred, forming a viscous, translucent gel. The increased water content in BP-2 and BP-3 samples has facilitated enhanced bubble formation, which contributed to internal foaming. Controlled physical foaming was induced by entrapped air bubbles due to continuous stirring and water vapor generation at elevated temperatures, as shown in Fig. 1(b), avoiding chemical blowing agents. The hot, foamed gel was immediately transferred into a preheated aluminum mold (dimensions: 10 × 10 × 0.5 cm^3) to preserve the pore structure. The molds were placed in a ventilated oven at 45 ± 2 °C for 48 h to allow slow evaporation of moisture and stabilization of pore morphology, as shown in Fig. 1(c). A slow drying rate with high ambient humidity ($R_H > 60$ %) was critical to prevent pore collapse and shrinkage. After drying, the bioplastic films were peeled off and conditioned at 25 ± 2 °C for 48 h before characterization as shown Fig. 1(d). The typical thickness of the films is in the range of 0.6–0.8 mm (measured using a screw gauge with an accuracy of 0.01 mm). As the water content increased across the three biodegradable plastic film samples (BP-1 to BP-3), the films became thinner, larger in size, softer in texture, and semi-translucent. The color shifted slightly from pale beige to yellowish-cream. These changes indicate that higher water content during film formation leads to better spreading, greater gelatinization, and more flexible films.

Instrumentation

The plastic nature of the prepared BP samples was studied by X-ray diffraction (XRD) spectra recorded using X-pert^3 diffractometer (Malvern Panalytical, Almelo, Netherlands) in the range of 10–70° with the resolution of 0.05 °C and scan time 10 min per sample. Scanning electron microscopy (SEM) images (magnification of 10,000× and resolution of 20 nm) and EDAX (energy dispersive X-ray analysis) profiles were recorded on TESCAN VEGA electron microscope (TESCAN, Brno, Czech Republic) at acceleration potential 15 kV. Fourier-transform spectrometer (FTIR) (Bruker-IFS 66 V, Bruker Corporation, Ettlingen, Germany) was used to identify the chemical bonds associated with functional groups of prepared BP samples in the range 400–4000 cm^{-1} with the resolution of 0.1 cm^{-1} and 20 scans per sample.

Extraction of porosity features

A hybrid image segmentation pipeline that combines deep learning and traditional image processing methods was used to assess the porosity properties of the biodegradable plastic samples. The scikit-image, numpy, and matplotlib libraries were used to implement the study in Python. In order to improve contrast and reduce background noise, adaptive thresholding (which calculates local thresholds for each pixel based on its neighbourhood) was initially used to preprocess SEM micrographs [18]. Subsequently, a U-Net based pore segmentation model was used to determine porosity parameters such as pore count (N), pore area (A), porosity (%), average pore size, circularity (C), and solidity (S') of the samples [19,20]. This model was refined using high-resolution datasets after being trained on manually annotated SEM images. Figure 2 shows a flowchart for obtaining porosity characteristics of the prepared BP samples. The flowchart demonstrates a hybrid image segmentation pipeline that integrates both classical image processing and deep learning techniques. The process begins with an input SEM image, which is first subjected to adaptive thresholding [18].

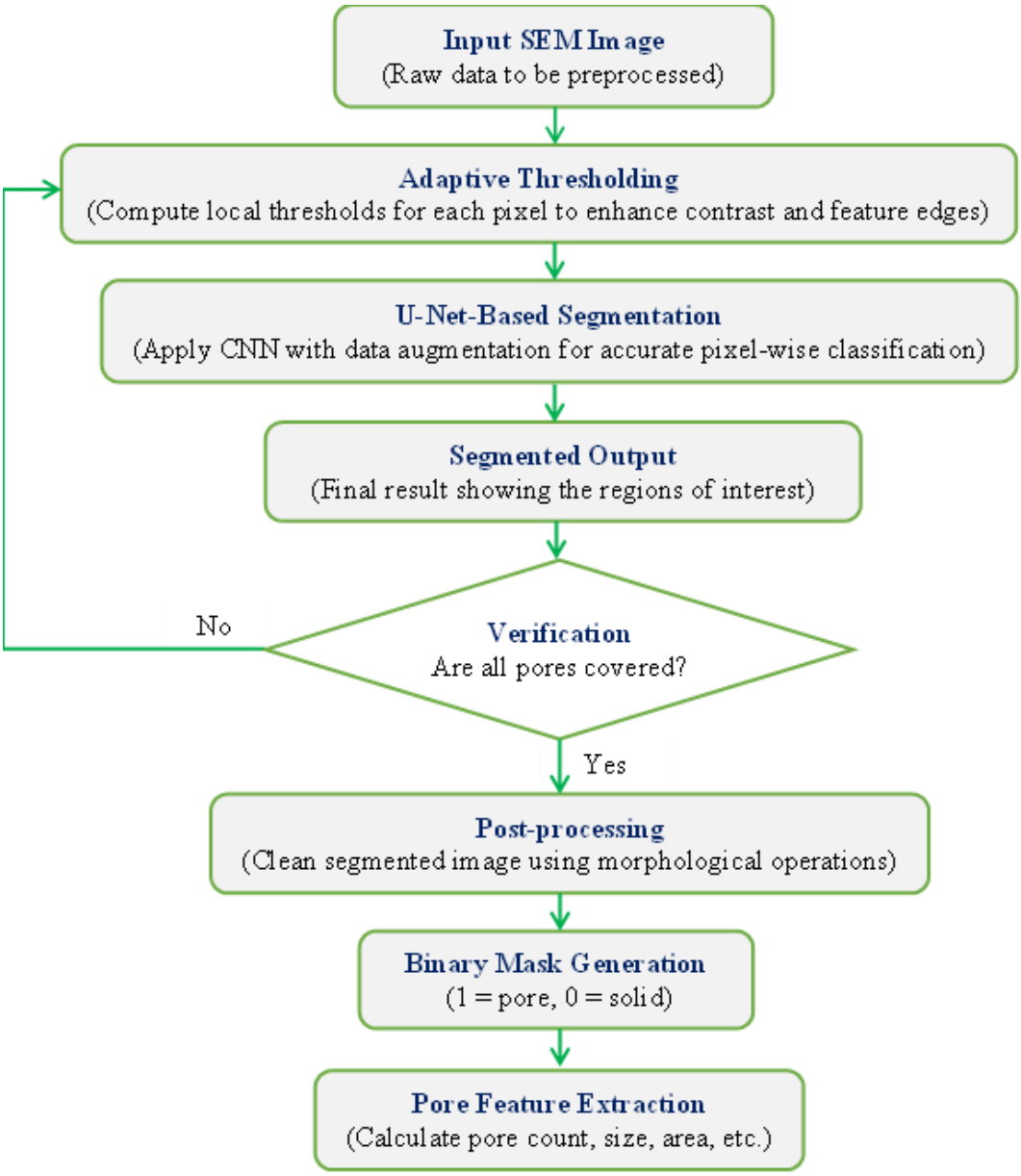


Fig. 2 Flowchart for obtaining porosity characteristics of the prepared BP samples

The adaptive thresholding technique is used to compute a threshold value locally for each pixel ($p > 0.6$) based on the surrounding neighbourhood and image inhomogeneities. This preprocessing step helps in enhancing important features and suppresses background noise. After thresholding the image, it is then passed to a U-Net-based segmentation model. During this stage, data augmentation techniques are applied to improve model generalization, and convolutional layers extract high-level features essential for accurate segmentation. Post-processing with morphological operations such as erosion, dilation, opening, closing, and hole-filling helps to refine the segmented image by removing noise, filling gaps, and smoothing boundaries. The cleaned segmentation is converted into a binary mask, where pores are represented by 1 s and solids by 0 s. Next, connected-component labelling assigns a unique color to each pore, allowing for the extraction of geometric features like pore count (N), pore area (A), porosity (%), average pore size, circularity (C), and solidity (S') [19,20].

Biodegradability test

The volume degradability of the prepared bioplastic films was measured by burying in red soil for a week (7 days), pouring 10 ml of water daily. A significant reduction in the size of the samples was observed, indicating notable degradation of the plastic films over time. Thus, the volume degradability of the samples is measured using Eq. (1):

$$Volume\ degradability\ (\%) = \left|\frac{V_f - V_i}{V_i}\right| \times 100, \quad (1)$$

where V_i and V_f are initial and final volume of the sample, and $(V_f - V_i)$ is the change in the volume after decomposition [3]. The sample dimensions were measured accurately after drying and cutting into rectangular shapes as shown in Fig. 1(d). The samples were immediately processed for the decomposition test immediately. Thus, there would not be any ambiguity in the correctness of the biodegradability test.

Results and Discussion

XRD and Crystallinity

X-ray diffraction patterns of the BP samples are displayed in Fig. 3. Prominent reflections at 2θ values of ≈15° (100), ≈17° (110), ≈18° (200), and ≈23° (300) indicate the A-type cereal starch signature, which is characteristic of native corn starch granules [3,21]. Instead of fundamental A-type lattice planes, Sample 2 exhibits an intense band at $2\theta \approx 20.01°$, which is typical of V-type single-helical amylose–lipid (such as glycerol, fatty acid) inclusion complexes formed during plasticization [21,22]. A small shoulder at $2\theta \approx 22°$ indicates the appearance of B-type or retrograded amylose domains, which are frequently seen in starch products that have gone through cycles of gelatinization and retrogradation [23,24].

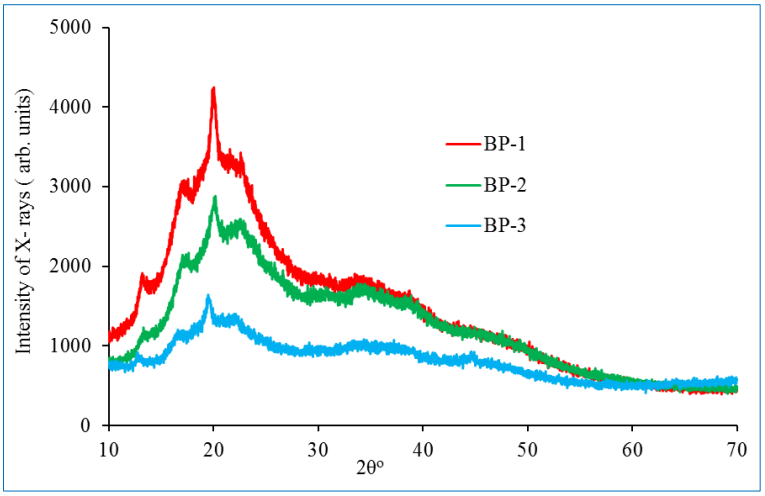


Fig. 3 XRD spectra of corn starch-based biodegradable plastics

The XRD patterns have displayed weak diffraction peaks and broader humps. This observation suggests that the samples have a partial crystalline nature. Usually, the partial crystallization in bioplastics could arise due to the irregular biopolymer structure influenced by the method of preparation, post processing, and environmental conditions. The vinegar (acetic acid) could lower the pH of the biopolymer composition,

which promotes more effective gelatinization of corn-starch during heating and facilitates the breakdown of intermolecular hydrogen bonds of the polymer mixture. The presence of plasticizers such as glycerine could further disrupt inter-molecular hydrogen bonding, thereby promoting amorphous regions associated with feeble crystallites. Thus, most of the starch-based bioplastics possess irregular chain architecture (amorphous) and heterogeneous crystallinity [25,26]. The degree of crystallinity (X_c) of three biodegradable plastic samples (BP-1, BP-2, and BP-3) is calculated from their XRD patterns using Eq. (2) [27]:

$$X_c = \left(\frac{A_c}{A_c + A_a}\right) x\ 100, \quad (2)$$

where A_c is the area under crystalline peaks (estimated around 15, 18, 20, 22, 23°), and A_a is the amorphous region (rest of the curve). The crystalline area (A_c) represents the portion of the XRD pattern corresponding to ordered crystalline regions, while the amorphous area (A_a) represents disordered non-crystalline regions. The degree of crystallinity (X_c) of the bioplastics was assessed as follows: a smooth curve connecting the crystallite peak baselines was drawn on the XRD pattern. The values of area above and under the smooth curve were evaluated corresponding to the crystalline (A_c) and the amorphous regions (A_a), respectively. The degree of crystallinity (X_c) was computed as a ratio between the area of the crystalline region (A_c) and the total area (A_c+A_a) under the XRD curve [28]. The degree of crystallinity (X_c) of the prepared corn starch-based biodegradable plastic films has followed the order: BP-1 > BP-2 > BP-3, as shown in Table 2. Among the three samples, BP-1 exhibits the highest crystallinity of 29.70 %, indicating a more ordered internal structure. The degree of crystallinity (X_c) of starch-based bioplastic films is strongly associated with their moisture content. Therefore, the higher value of the degree of crystallinity of BP-1 sample (as shown in Table 2) is compatible with the lower moisture content [29]. The sample BP-2 has 24.47 % crystallinity, while the sample BP-3 has the lowest crystallinity 20.87%. This trend confirms that more absorption of water content from sample BP-1 to sample BP-3. Thus, disruption of hydrogen bonds would build weak polymer chains with poor crystallinity in the sample BP-3 [3,21].

Table 2. Degree of crystallinity (X_c) of three biodegradable plastic samples

Sample	Crystalline area (A_c) (X-ray intensity x 2θ) arbitrary units	Amorphous area (A_a) (X-ray intensity x 2θ) arbitrary units	X_c, %
BP-1	26,047.58	61,669.38	29.70
BP-2	18,284.78	56,446.21	24.47
BP-3	10,211.71	38,723.27	20.87

SEM and porosity

Figure 4(a–c) displays the SEM morphographs of the bioplastics BP-1, BP-2, and BP-3. SEM images have clearly reflected partial heterogeneous crystalline nature along with homogeneous amorphous nature as observed in the XRD analysis. The crystallinity could enhance mechanical rigidity, while the amorphous phase would contribute to the ductility of the samples. Such structural modifications indicate a good balance between strength and flexibility of the samples [8,14]. A few residual granules and insoluble fragments are

presented, which indicate incomplete gelatinization during the preparation [30]. The SEM micrographs have shown distinct surface morphologies for the three samples. The sample BP-1 has displayed a very smooth and good compact surface with a very fine and uniformly distributed grains (of size ~ 1–10 μm), which depicts a well-structured material with a higher crystalline phase. The SEM image of the sample BP-2 has appeared slightly rough with visible microcracks (of size ~ 5–20 μm) and discrete particulates (of size ~ 5–15 μm), which suggests a moderate structural order and partial phase separation of crystallinity.

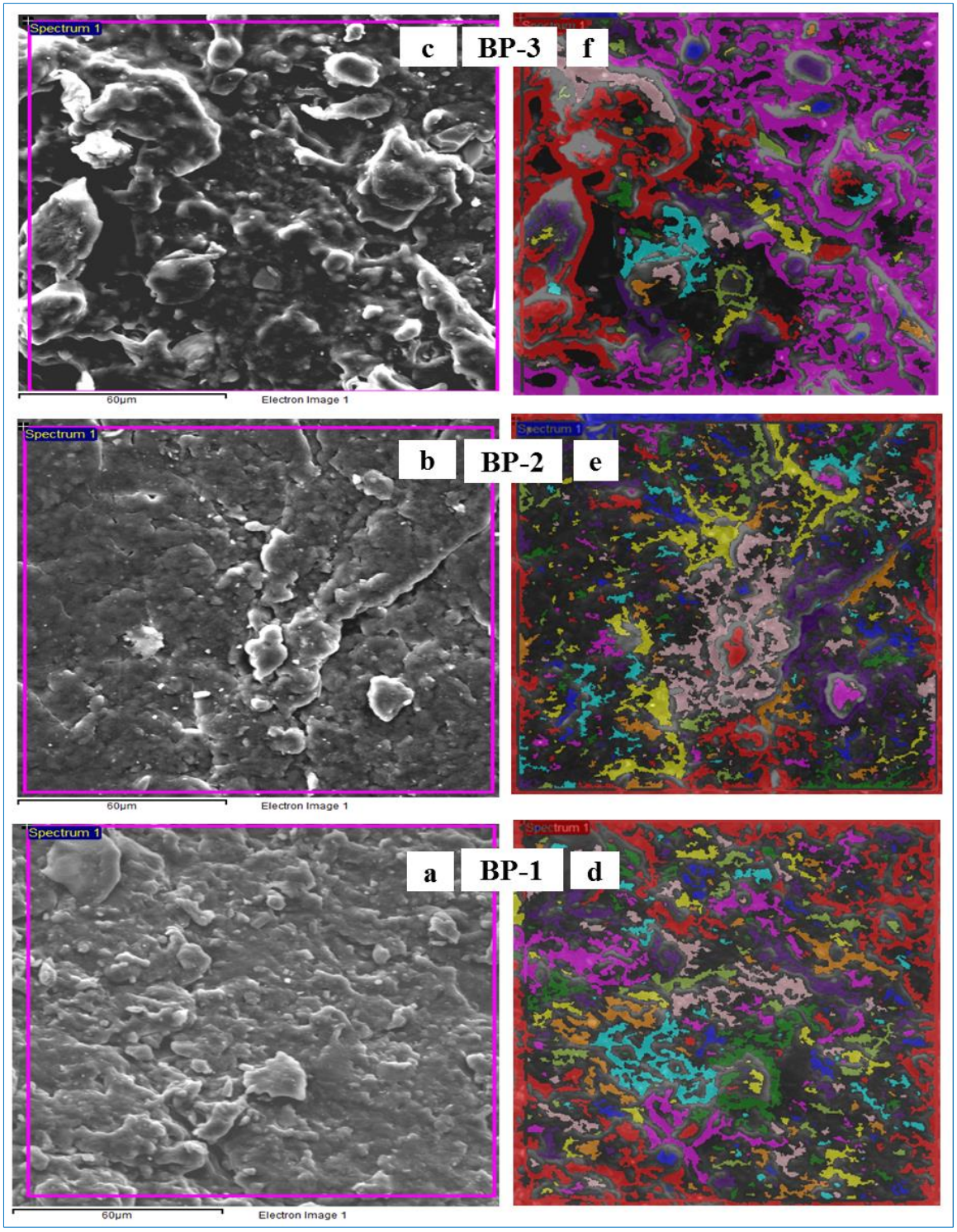


Fig. 4 SEM morphographs (a), (b), and (c) with corresponding pore segmentation overlays (d), (e), and (f) of biodegradable plastic samples BP-1, BP-2, and BP-3 respectively

The SEM image of sample BP-3 has revealed a highly rough surface and more porous surface with larger voids and aggregates (of size ~ 10–30 μm), which represents poor polymer networking and a more amorphous phase [30,31]. These observations are in agreement with the XRD data, which has shown a gradual increase in amorphous nature of the samples in the order: BP-1 < BP-1 < BP-3 as water content increases in the composition.

Figure 4(d–f) displays the pore segmentation in SEM micrographs of the samples BP-1, BP-2, and BP-3, using adaptive thresholding and U-Net model [18–20]. The porosity parameters are shown in Table 3. The sample BP-1 has exhibited the highest number of pores ($N = 528$) with the smallest values of porosity (24.26 %) and average pore size (119.74 μm^2), showing a compact structure. The sample BP-3 has displayed the lowest number of pores ($N = 128$) with the highest values of porosity (31.67 %) and average pore size (585.52 μm^2), exhibiting a loosely packed and amorphous structure [18,32,33]. This viewpoint suggests that increased water content could promote the formation and amalgamation of larger pores in the bioplastics. Circularity (C) values are observed to be less than unity ($C < 1$) for all the samples. However, $C \approx 1$ for the sample BP-1 shows the most circular pore shapes. Solidity (S') is observed in the order: BP-1 > BP-2 > BP-3, showing a higher degree of wider and irregular pore boundaries with an increase in water content in the composition [34,35].

Table 3. Porosity characteristics of corn starch based biodegradable plastics

Sample	Pore count (N)	Total pore area, μm²	Porosity, %	Avg. pore size, μm²	Circularity (C)	Solidity (S')
BP-1	528	63,233	24.26	119.74	0.925	0.760
BP-2	419	68,414	26.72	163.30	0.890	0.746
BP-3	128	74,946	31.67	585.52	0.865	0.742

EDAX and elemental analysis

Figure 5 displays the EDAX spectra of the bioplastic samples BP-1, BP-2, and BP-3. The EDAX analysis has confirmed the presence of constituent elements such as carbon (C), oxygen (O), calcium (Ca), magnesium (Mg), silicon (Si), aluminium (Al), chlorine (Cl), and sodium (Na) [36,37]. The presence of these elements indicates the organic nature of the prepared bioplastics. These elements are fundamental components of the polysaccharides (amylose and amylopectin), which could form the primary polymer structure of cornstarch. The weight% and atomic% of the elements are presented in Table 4.

The peaks due to the elements carbon (C), oxygen (O), and calcium (Ca) are predominant in all three samples. The sample BP-1 has shown peaks attributed to Fe and Mg, suggesting the presence of a higher number of inorganic residues. The sample BP-2 has displayed a uniform distribution of elements Mg, Al, Si, and Cl with low-intense peaks. The presence of Cl suggests modest mineral-based impurities in the sample BP-2. The sample BP-3 has presented the significant peaks attributed to elements Na and Cl, due to the presence of higher water content in the composition. This water (moisture) could increase the mobility of these ions within the bioplastic matrix. Notably, Fe and Mg peaks are absent in the sample BP-3, which indicates that the sample BP-3 has lower inorganic content for enhancing decomposition of the bioplastic [36,37].

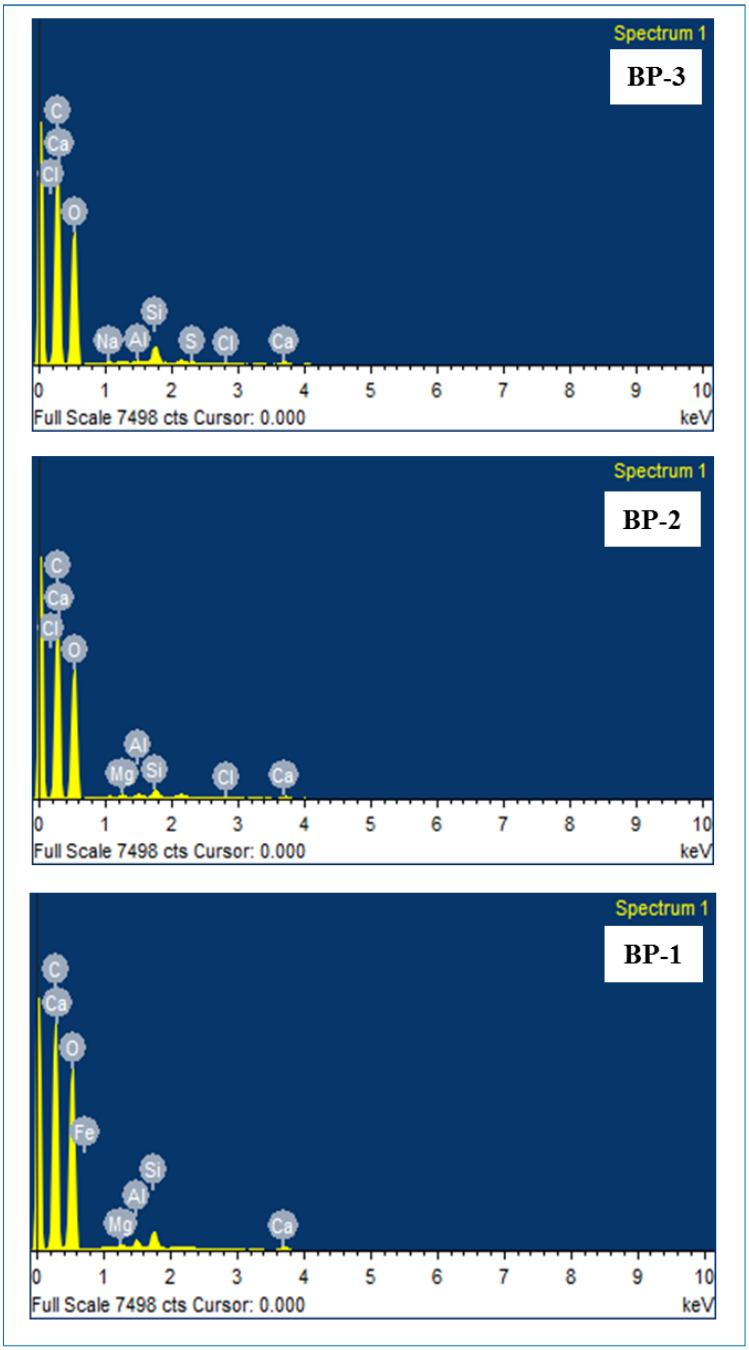


Fig. 5. EDAX spectra corn based of biodegradable plastic samples BP-1, BP-2, and BP-3

Table 4. EDAX analysis of the corn-starch biodegradable plastics

BP-1			BP-2			BP-3		
Element	**Wt. %**	**At. %**	**Element**	**Wt. %**	**At. %**	**Element**	**Wt. %**	**At. %**
C	45.79	53.62	C	47.17	54.78	C	48.41	56.25
O	51.22	45.03	O	50.81	44.30	O	48.52	42.32
Mg	0.26	0.15	Mg	0.21	0.12	Na	0.25	0.15
Al	0.52	0.27	Al	0.25	0.13	Al	0.21	0.11
Si	1.27	0.64	Si	0.79	0.39	Si	1.61	0.80
Ca	0.58	0.20	Cl	0.25	0.10	S	0.08	0.04
Fe	0.36	0.09	Ca	0.52	0.18	Cl	0.22	0.09
-	-	-	-	-	-	Ca	0.70	0.24
Total	100	100	Total	100	100	Total	100	100

FTIR and structure

Figure 6 shows FTIR spectra of the corn-starch bioplastics. The FTIR spectra have revealed distinct transmission bands corresponding to various polymer groups as reported in [21,29,31]. The hydroxyl (O–H) stretching vibrations have been identified at ~ 3340–3365 cm^{-1}, confirming the network of O–H bonds in starch, water, and glycerine. Carbonyl C–H stretching (aliphatic) vibrations are resolved at ~ 2955–2965 cm^{-1}. The C=O stretching bands of functional groups of acetic acid and ester have been noticed at ~ 1717–1735 cm^{-1}. The H–O–H stretching vibrations are observed to ~ 1610–1625 cm^{-1}. The CH_2 bending or COO^- symmetric stretching vibrations are attributed at ~ 1428–1439 cm^{-1}. The stretching vibrations of C–O–C bonds are noticed at ~ 1090–1102 cm^{-1}, which are characteristic bands of polysaccharide structures. Vibrations due to deformation of α-1,4 glycosidic linkages in corn starch are revealed at ~ 917–926 cm^{-1}. Moreover, deformation of C–H bonds have been observed at ~783–820 cm^{-1}. The presence of observed bands could confirm the plastic nature of the prepared samples [21,29,31].

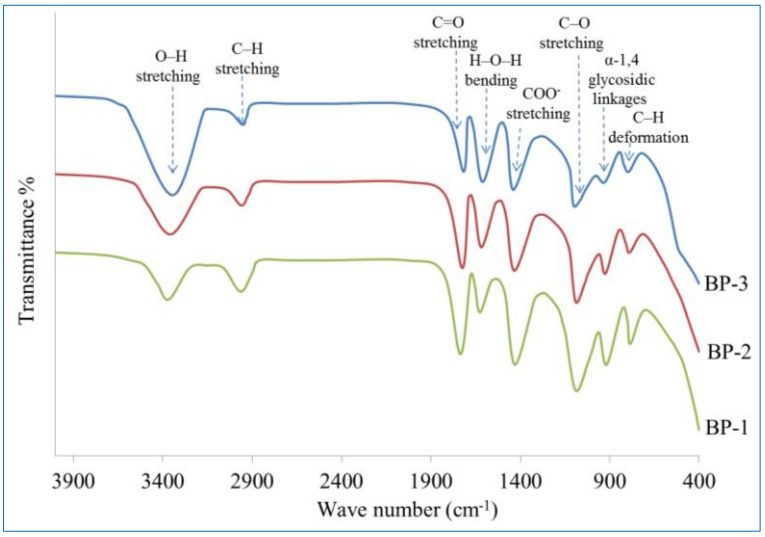


Fig. 6. FTIR spectra of corn based biodegradable plastics

The intensity of hydroxyl (O–H and O–H–O) groups have gradually increased from BP-1 to BP-3, at simultaneous reduction of intensity of carbonyl (C=O, COO^-, and C–O–C) groups. The increase in intensity of hydroxyl groups can be attributed to the higher proportion of water in the composition. Moreover, in the presence of vinegar (acetic acid) in the composition, water molecules could slightly change the corn-starch structure. Consequently, an increase in available hydroxyl groups is observed in the sample BP-3. At the same time, the gradual decrease in intensity of carbonyl bands suggests a reduction in esters or oxidized groups. Thus, the observed structural modifications in the bioplastics confirm the crucial role of water (H_2O) in the composition [21,34].

Decomposition

The samples have been processed with a decomposition test for 7 days in atmospheric conditions with room temperature (t_r) ~ 25–35 °C and humidity (R_H) ~ 55–65 %. After 7 days of burial in red soil with consistent moisture maintained by the daily addition of

10 ml of water, the BP-1, BP-2, and BP-3 biodegradable plastic samples showed clear signs of decomposition (as shown in Fig. 7), influenced by their water content and initial porosity [16,21]. After 7 days, the area and thickness of the samples are found to be significantly decreased. Thus, the decomposition of the prepared cornstarch biodegradable plastics in the red soil has been determined [3]. Volume degradability of the BP-1, BP-2, and BP-3 samples is presented in Table 5.

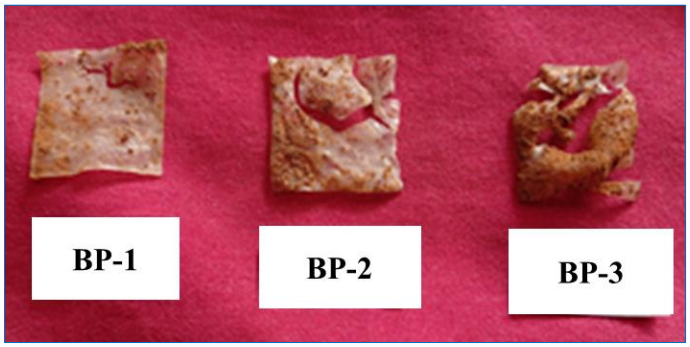


Fig. 7. Decomposition of the prepared biodegradable plastics

Table 5. Volume degradation of the prepared cornstarch biodegradable plastic samples

Sample	Volume (V_i), cm^3	Volume (V_f), cm^3	Volume degradability, %
BP-1	0.407	0.301	26.044
BP-2	0.645	0.260	59.690
BP-3	0.726	0.114	84.298

The sample BP-3exhibited the most significant degradation (84.298 %) with higher surface erosion and significant disintegration [38]. This degradation behavior could be attributed to faster microbial infiltration and hydrolytic activity by the higher amorphous phase and large pore size of the sample BP-3 [39]. The sample BP-2 has showed moderate decomposition (59.690 %), with a clear surface cracking and micro-patching. The moderate crystallinity and structural disorder could allow microbial and moisture penetration in the sample BP-2. The sample BP-1 has shown the least degradation (26.044 %) with a small crack and minor patches, having the most crystalline and structurally compact with the lowest porosity. Thus, the rate of degradation depends on moisture retention, porosity, and crystallinity of the bioplastics [40,41]. These findings indicate that higher water content in the initial composition improves biodegradability [3,16,21,38,39].

Potential applications and future scope

The corn-starch biodegradable plastics have become promising materials for practical applications. These bioplastic materials can exhibit good flexibility due to the presence of α-1,4-glycosidic linkages, hydroxyl and carbonyl functional groups. The present corn-starch bioplastics have shown a reasonably good decomposition in the range of ~ 25–86 % in the soil environment, which is on par with the standards of ASTM (American Society for Testing and Materials) for compostable plastics (code: D6400) and other international agencies [42]. These bioplastics can be especially suitable for single-use packing applications such as biodegradable bags, food wrapping films, and disposable containers [7,8,10]. Moreover, these bioplastics are ideal candidates for manufacturing agricultural

mulch films, which can be decomposed naturally in soil environments, promoting the soil health [43]. In this way, corn-starch biodegradable plastics showcase significant versatility and act as alternatives for use of petroleum-based plastics in daily life applications [39,43]. Future research on corn-based biodegradable plastics can be focused on enhancement of mechanical strength, water resistance, and thermal stability by means of chemical modification or blending with other biopolymers [43]. Moreover, exploration of industrial-scale production and decomposition nature of the bioplastics under real-world conditions will find a wide range of applications in packing, agriculture, and biomedical fields [43–47].

Conclusion

Three corn starch-based biodegradable plastics (BP-1, BP-2, and BP-3) were synthesized via solvent casting combined with a controlled physical foaming process. The microstructural, structural, and decomposition studies have been carried out. The scientific findings are listed as follows:

1. X-ray diffraction (XRD) analysis revealed a homogeneous amorphous state of the samples associated with partial heterogeneous crystallites. The degree of crystallinity (X_c) of the prepared corn starch-based biodegradable plastic films has followed the order: BP-1 > BP-2 > BP-3. Gradual loss of native crystallinity with increasing water content, suggesting enhanced amorphous character and improved flexibility in the sample BP-3.
2. SEM morphology of the sample BP-1 displayed a smooth and compact surface with evenly distributed fine granules, indicating a well-structured and dense material, consistent with a higher crystalline nature. Porosity measurements revealed increased pore size and volume with higher water content, contributing to improved water absorption and biodegradability from BP-1 to BP-3. Circularity (C) values were observed to be less than 1 for all the samples, with BP-1 having the most regular pore shapes. Solidity (S') followed the order BP-1 > BP-2 > BP-3, indicating increasing irregularity of pore boundaries as water content increases.
3. Energy-dispersive analysis by X-rays (EDAX) confirmed the elemental composition of the bioplastic samples, primarily showing the presence of carbon and oxygen, which is consistent with the starch-based polymer matrix.
4. FTIR analysis showed that O–H band intensity increased and C=O band intensity decreased from BP-1 to BP-3, suggesting more hydroxyl groups and fewer carbonyl groups as water content increased in the composition.
5. Decomposition rate has increased due to enhanced hydrolysis and microbial activity with high water content in the composition and high porosity of the samples. Therefore, these bioplastics can have applications in packing, agricultural mulch-films, and disposable products.

However, the corn-starch bioplastics have several important limitations, including high moisture absorbance and poor mechanical strength, which can diminish their performance. Also, variations in the composition of raw materials and synthesizing methods may lead to unreliable quality and thickness. Yet, large-scale production of the bioplastics is costly. All these issues can be addressed by developing water-resistant plastic coatings, inexpensive ingredients, and standardized synthesis methods, which will help to make the corn-starch bioplastics highly reliable and suitable for practical applications in daily life.

CRediT authorship contribution statement

Linganaboina Srinivasa Rao: conceptualization, methodology, investigation, formal analysis, validation, resources, supervision, writing – review & editing, writing – original draft; **Jyotsna Cherukuri:** methodology, investigation, formal analysis, validation, writing – review & editing; **Nalimela Pothanna:** methodology, investigation, formal analysis, validation; **Redrowthu Vijaya Saraswathi**: conceptualization, methodology, resources, software; **Linganaboina Prabhatha Sindu Sri:** methodology, data curation, software; **Sahith Battula**: methodology, investigation, data curation, writing – review & editing, writing – original draft.

Conflict of interest

The authors declare that they have no conflict of interest.

References

1. Houssini K, Li J, Tan Q. Complexities of the global plastics supply chain revealed in a trade-linked material flow analysis. *Commun Earth Environ.* 2025;6: 257.
2. Kapustin NO, Grushevenko DA. Analysis of the "circular plastics economy" phenomena and its long-term implications for demand for petroleum market. *Environ Sci Pollut Res.* 2023;30: 85889–85902.
3. Srinivasa Rao L, Naidu CD, Tiwari S. Investigation on synthesis, structure and degradability of starch based bioplastics. *Mater Today Proc.* 2022;49: 257–261.
4. Hossain MT, Shahid MA, Akter S, Ferdous J, Afroz K, Refat KRI, Faruk O, Jamal MSI, Uddin MN, Samad MAB. Cellulose and starch-based bioplastics: a review of advances and challenges for sustainability. *Polym-Plast Technol Mater.* 2024;63(10): 1329–1349.
5. Jiang S, Wang S, Peng G, Qiao C, Yao J. Structural Characterization and Properties of Deep Eutectic Solvents Plasticized Chitosan Films. *J Macromol Sci Part B Phys.* 2024;63(6): 461–477.
6. Akshaykranth A, Jayarambabu N, Kumar A, Venkatappa Rao T, Rakesh Kumar R, Srinivasa Rao L. Novel nanocomposite polylactic acid films with Curcumin-ZnO: structural, thermal, optical and antibacterial properties. *Curr Res Green Sustainable Chem.* 2022;5: 100332.
7. Akshaykranth A, Jayarambabu N, Venkatappa Rao T, Rakesh Kumar R, Srinivasa Rao L. Antibacterial activity study of ZnO incorporated biodegradable poly (lactic acid) films for food packaging applications. *Polym Bull.* 2023;80: 1369–1384.
8. Kowser MA, Mahmud H, Chowdhury MA, Hossain N, Mim JJ, Islam S. Fabrication and characterization of corn starch based bioplastic for packaging applications. *Results Mater.* 2025;25: 100662.
9. Safira NP, Heryanto H, Tahir D, Syam F, Akouibaa A. Development and characterization of cornstarch-based bioplastics: Influence of fructose concentration and titanium dioxide (TiO_2) variations on structural, chemical bonding, and nutrient-related properties of mung bean plants. *Int J Biol Macromol.* 2024;283: 137852.
10. Aguilar-Palazuelos E, Fitch-Vargas PR, Delgado-Nieblas CI, López-Diaz A, Gastélum-Ávila A, Sánchez-Chilero MA, Limón-Valenzuela, V, Camacho-Hernández IL, Ruiz-Armenta XA, Calderón-Castro A. Edible Films Based on Corn Starch and Gelatin Obtained by the Combination of Extrusion and Casting Process: Characterization and Applications. *Food Biophys.* 2025;20: 2.
11. Patnaik S, Panda AK, Kumar S. Thermal degradation of corn starch based biodegradable plastic plates and determination of kinetic parameters by isoconversional methods using thermogravimetric analyzer. *J Energy Inst.* 2020;93(4): 1449–1459.
12. Sedayu BB, Jatmiko VA, Fransiska D, Abdullah AHD, Nissa RC, Hakim AR, Fauzi A, Nur M. Characteristics of Carrageenan/Corn Starch Biodegradable Plastic Films Produced by Extrusion Blending. *Waste Biomass Valor.* 2025;16: 5873–5883.
13. Wang B, Yu B, Yuan C, Guo L, Liu P, Gao W, Li D, Cui B, Abd El-Aty AM. An overview on plasticized biodegradable corn starch-based films: the physicochemical properties and gelatinization process. *Crit Rev Food Sci Nutr.* 2022;62(10): 2569–2579.

14. Jayalath UT, Samaraweera H, Samarasinghe A. Development and characterization of gelatin-starch bioplastics: A comparative study of cassava, corn, and rice-based alternatives. *Sustainable Chem Environ.* 2025;9: 100190.
15. Soykeabkaew N, Thanomsilp C, Suwantong O. A review: Starch-based composite foams. *Compos Part A.* 2015;78: 246–263.
16. Singh P, Pandey VK, Singh R, Singh K, Dash KK, Malik S. Unveiling the potential of starch-blended biodegradable polymers for substantializing the eco-friendly innovations. *J Agric Food Res.* 2024;15: 101065.
17. Peng Y, Wu Y, Shan Z, Wen X, Li M, Ni Y. Preparation and Characterization of Corn Starch Fractions from Varied Zein Extraction Processes: Implications for Industrial Structure Adjustment. *Food Bioprocess Technol.* 2025;18: 7661–7676.
18. Sahith B, Nived A, Sri Sai Pavan M, Srinivasa Rao L, Chennakesava Rao B. Morphological Insights of Lithium-Phosphate Nano Compounds by Data Driven Pore Analysis of SEM Images with ML Algorithms. *Indian J Sci Technol.* 2025;18(1): 72–80.
19. Ronneberger O, Fischer P, Brox T. U-Net: Convolutional Networks for Biomedical Image Segmentation. In: Navab N, Hornegger J, Wells W, Frangi A. (Eds) *Medical Image Computing and Computer-Assisted Intervention – MICCAI 2015. Lect Notes Comput Sci., vol 9351.* Cham: Springer; 2015. p.234–241.
20. Sagar BS, Wang C, Zhou X, Hassan M. Scanning electron microscopy (SEM) image segmentation for microstructure analysis of concrete using U-net convolutional neural network. *Autom Constr.* 2022;144: 104602.
21. Lounis FM, Benhacine F, Hadj-Hamou AS. Improving water barrier properties of starch based bioplastics by lignocellulosic biomass addition: Synthesis, characterization and antibacterial properties. *Int J Biol Macromol.* 2024;283: 137823.
22. Malmir S, Montero B, Rico M, Barral L, Bouza R, Farrag Y. Effects of poly (3-hydroxybutyrate-co-3-hydroxyvalerate) microparticles on morphological, mechanical, thermal, and barrier properties in thermoplastic potato starch films. *Carbohydr Polym.* 2018;194: 357–364.
23. Haixia Z, Zhiguang C, Junrong H, Huayin P. Exploration of the process and mechanism of magnesium chloride induced starch gelatinization. *Int J Biol Macromol.* 2022;205: 118–127.
24. Surendren A, Mohanty AK, Liuc Q, Misra M. A review of biodegradable thermoplastic starches, their blends and composites: recent developments and opportunities for single-use plastic packaging alternatives. *Green Chem.* 2022;24(22): 8606–8636.
25. Stanley J, Poulain C, Debeaufort F, Brachais C, Culliton D, Benbettaieb N, Jovani-Sancho A, Neves AC. Material characterisation of bioplastics: Influence of different starch sources in fish gelatin-based blends. *Materials Today Sustainability.* 2026;34: 101344.
26. Mukurumbira A, Mariano M, Dufresne A, Mellem JJ, Amonsou EO. Microstructure, thermal properties and crystallinity of amadumbe starch nanocrystals. *Int J Biol Macromol.* 2017;102: 241–247.
27. Nara S, Komiya T. Studies on the Relationship Between Water-satured State and Crystallinity by the Diffraction Method for Moistened Potato Starch. *Starch.* 1983;35(12): 407–410.
28. Dome K, Podgorbunskikh E, Bychkov A, Lomovsky O. Changes in the Crystallinity Degree of Starch Having Different Types of Crystal Structure after Mechanical Pretreatment. *Polymers.* 2020;12(3): 641.
29. Ibrahim MIJ, Sapuan SM, Zainudin ES, Zuhri MYM. Physical, thermal, morphological, and tensile properties of cornstarch-based films as affected by different plasticizers. *Int J Food Prop.* 2019;22(1): 925–931.
30. Amin MR, Chowdhury MA, Kowser MA. Characterization and performance analysis of composite bioplastics synthesized using titanium dioxide nanoparticles with corn starch. *Heliyon.* 2019;5(8): e02009.
31. Rajesh Y, Gautam N, Saloni P, Deore V, Shivde P, Dabhade G. Agricultural resources in focus: Eco-friendly bioplastic synthesis from corn starch. *Mater Today Proc.* 2024;111: 182–187.
32. Hojat N, Gentile P, Ferreira AM, Šiller L. Automatic pore size measurements from scanning electron microscopy images of porous scaffolds. *J Porous Mater.* 2023;30: 93–101.
33. Fang X, Wang C, Li H, Wang X, Zhang S, Luo X, Jia H. Influence of mesoscopic pore characteristics on the splitting-tensile strength of cellular concrete through deep-learning based image segmentation. *Constr Build Mater.* 2022;315: 125335.
34. Alonso-González M, Felix M, Romero A. Development of rice bran-based bioplastics via injection molding: Influence of particle size and glycerol ratio. *Resour Conserv Recycl.* 2024;208: 107713.
35. Nandiyanto ABD, Fiandini M, Ragadhita R, Sukmafitri A, Salam H, Triawan F. mechanical and biodegradation properties of cornstarch-based bioplastic material. *Materials Physics and Mechanics.* 2020;44(3): 380–391.

36. Selvaraj K, Vishvanathan N, Dhandapani R. Screening, optimization and characterization of poly hydroxy butyrate from fresh water microalgal isolates. *Int J Biobased Plast.* 2021;3(1): 139–162.
37. Kamal M, Shukla S. IR, SEM and EDX/EDS analysis of Starch and Coniferyl Alcohol-based polymer with other natural additives. *Essential Chem.* 2025;2(1): 1–8.
38. Anubha M, Saranya R, Chandrasatheesh C, Jayapriya J. Effect of neem gum on water sorption, biodegradability and mechanical properties of thermoplastic corn starch-based packaging films. *Indian Chem Eng.* 2022;64(5): 594–606.
39. Omura T, Isobe N, Miura T, Miura T, Ishii S, Mori M, Ishitani Y, Kimura S, Hidaka K, Komiyama K, Suzuki M, Kasuya K, Nomaki H, Nakajima R, Tsuchiya M, Kawagucci S, Mori H, Nakayama A, Kunioka M, Kamino K, Iwata T. Microbial decomposition of biodegradable plastics on the deep-sea floor. *Nat Commun.* 2024;15: 568.
40. Soler A, Velazquez G, Velazquez-Castillo R, Morales-Sanchez E, Osorio-Diaz P, Mendez-Montealvo G. Retrogradation of autoclaved corn starches: Effect of water content on the resistant starch formation and structure. *Carbohydr Res.* 2020;497: 108137.
41. Triawan F, Nandiyanto ABD, Suryani I O, Fiandini M, Budiman B A. The influence of turmeric microparticles amount on the mechanical and biodegradation properties of cornstarch-based bioplastic material: from bioplastic literature review to experiments. *Materials Physics and Mechanics.* 2020;46(1): 99–114.
42. Nizamuddin S, Baloch AJ, Chen C, Arif M, Mubarak NM. Bio-based plastics, biodegradable plastics, and compostable plastics: biodegradation mechanism, biodegradability standards and environmental stratagem. *Int. Biodeterior. Biodegrad.* 2024;195: 105887.
43. Yang N, Sun ZX, Feng LS, Zheng MZ, Chi DC, Meng WZ, Hou ZY, Bai W, Li KY. Plastic Film Mulching for Water-Efficient Agricultural Applications and Degradable Films Materials Development Research. *Mater Manuf Process.* 2014;30(2): 143–154.
44. Mokaddem A, Belkheir M, Rouissat M, Doumi B, Boutaous A. Interface shear damage of novel biocomposite materials based on polyhydroxyalkanoates biopolymer matrix. *Materials Physics and Mechanics.* 2024;52(4): 100–113.
45. Eslahi N, Mahmoodi A, Mahmoudi N, Zandi N, Simchi A. Processing and Properties of Nanofibrous Bacterial Cellulose-Containing Polymer Composites: A Review of Recent Advances for Biomedical Applications. *Polym Rev.* 2019;60(1): 144–170.
46. Reshmy R, Philip E, Thomas D, Madhavan A, Sindhu R, Binod P, Varjani, S, Awasthi, MK, Pandey, A. Bacterial nanocellulose: engineering, production, and applications. *Bioengineered.* 2021;12(2): 11463–11483.
47. Chinta ML, Gandam PK, Sivasankar MV, Parcha SR. Tamarind (Tamarindus indica L.) Seed Polysaccharide: A promising biopolymer for drug delivery, wound healing, tissue engineering and beyond. *Carbohydr Res.* 2025;552: 109454.